Materials Advances

ROYAL SOCIETY OF CHEMISTRY

PAPER

View Article Online
View Journal | View Issue

Cite this: *Mater. Adv.*, 2026, 7, 2882

Masterbatch strategy for enhanced filler dispersion and reinforcement of zirconia-filled NBR composites

Shubham C. Ambilkar, [ab] Surabhi S. Raut, [a] Bharat P. Kapgate[c] and Chayan Das *[a]

The reinforcement of elastomeric composites by inorganic non-black fillers such as metal oxides is primarily governed by their shape, size, and state of dispersion. However, the filler incorporation technique can also play a critical role in this regard. This study investigates the efficacy of a masterbatch approach for *in situ* zirconia reinforced nitrile butadiene rubber (NBR) composites. A comprehensive characterization of all the composites is carried out, including evaluation of their rheological, thermal, mechanical, morphological and dynamic mechanical properties. This approach is found to be very efficient in strengthening composite properties, such as enhancements in their mechanical and thermal properties, along with other properties like aging resistance, viscoelastic behaviour and compression set. The masterbatch-derived 20 phr zirconia containing NBR composite shows better performance than externally filled zirconia-NBR composite at the same filler content. The masterbatch approach ensures superior filler dispersion and enhanced interfacial interaction. Beyond performance metrics, this method represents a greener approach by reducing solvent usage and energy input with respect to the purely sol–gel derived *in situ* filler incorporation method, aligning with sustainable development goals and promoting eco-friendly material processing.

Received 20th September 2025,
Accepted 26th January 2026

DOI: 10.1039/d5ma01078k

rsc.li/materials-advances

1. Introduction

The reinforcement of rubber by adding a suitable reinforcing filler is a key step in achieving the desired mechanical properties and other strength-related properties in the composites to make them suitable for various commercial applications.[1,2] In recent times, the range of fillers for reinforcing rubber composites has been extended from widely used carbon black (CB) to other non-black fillers.[3–5] Among the inorganic non-black fillers, silica is highly recognized for its superior trade-off in terms of fuel efficiency and wet handling ability due to a smaller rolling loss compared to rubber composites filled with CB.[6,7] Titania and alumina also offer a number of advantageous properties in addition to notable reinforcement efficiency.[8–10] Zirconia is another emerging potential filler in the area of rubber composites because of its multiple advantages, including its biocompatibility, thermal stability and rigidity.[11–14] Although significant interest has been devoted to alumina and titania-based rubber composites, interest in zirconia has been limited. However, the incorporation of these metal oxides into elastomeric matrices with a very good state of dispersion remains challenging due to their strong interparticle interaction, high surface energy, and lack of compatibility with organic rubber matrices.[15–17] Among the various strategies that have been attempted to overcome this issue, surface modification of fillers by suitable coupling agents (mostly organosilanes) remains very successful.[18–20] Another highly effective approach involves the *in situ* sol–gel generation of inorganic oxide particles within the rubber matrix. In this process, the formation of the filler phase in the presence of polymer chains promotes strong interfacial interactions and uniform dispersion.[21–24]

In recent past, our group has reported several works using this method, in which *in situ* generated zirconia in the rubber matrix has proven to be an excellent reinforcing filler for various rubber and rubber blend composites.[13,14,16,19,25] However, these approaches typically rely on solvent assistance or latex-based solution assistance with prolonged reaction time, which limit their industrial applicability. To address these limitations, the masterbatch approach seems to be an effective alternative, enabling the transfer of sol–gel derived dispersion

[a] *Department of Chemistry, Visvesvaraya National Institute of Technology, Nagpur, Maharashtra 440010, India. E-mail: chayandas@chm.vnit.ac.in, chayandas@hotmail.com*
[b] *Department of Chemistry, Dhote Bandhu Science College, Gondia, Maharashtra 441614, India*
[c] *Indian Rubber Materials Research Institute, Thane, Mumbai, Maharashtra 400604, India*

quality into conventional rubber compounding routes while improving processability and scalability.[26] In this approach, the filler is predispersed at a high concentration in a polymer carrier or rubber latex and subsequently incorporated during compounding. This results in improved filler distribution, enhanced process control and more consistent product quality.[26–28]

A considerable number of studies have reported masterbatch-based strategies in which a pre-synthesized, unvulcanized elastomer masterbatch is used as a stock and subsequently blended with raw rubber in appropriate proportions to obtain composites with optimized formulations and tailored properties. This approach has been successfully adopted for various elastomers including natural rubber (NR),[29,30] styrene-butadiene rubber (SBR),[31,32] epoxidized natural rubber (ENR)[28] and nitrile butadiene rubber (NBR),[33] to incorporate diverse filler systems such as graphene,[29] silica,[30] clay,[31] lignin,[28] and carbon black[32] through wet mixing, solution compounding, melt mixing, or latex compounding routes, leading to significant enhancements in the mechanical properties and other functional properties of rubber composites.[28–32] In terms of NBR specifically, Balachandran *et al.* prepared NBR-nanocalcium carbonate (NCC) composites using an internal mixing-based masterbatch approach followed by two-roll milling. Improved filler dispersion resulted in superior mechanical, dynamic mechanical, thermal, and barrier properties compared with NBR-NCC composites; however, higher NCC loadings led to aggregation-induced performance deterioration.[33] The same group extended this masterbatch-based approach to NBR-nanoclay nanocomposites prepared *via* a two-stage compounding process, which significantly influenced their mechanical, dynamic mechanical, and thermal properties, including solvent sorption and gas permeation behavior.[34] Zhou *et al.* reported that ultra-high molecular weight polyethylene and graphite fluoride emerged as the most effective fillers, exhibiting superior tribological performance among the fillers studied.[35]

In light of this background, we have integrated a masterbatch strategy with *in situ* zirconia loading in NBR. Initially, an unvulcanized NBR masterbatch containing a high zirconia loading (40 phr) is prepared *via in situ* incorporation of zirconia. This masterbatch is subsequently blended with raw NBR in appropriate proportions to systematically dilute the filler content and then vulcanized to yield composites with the desired zirconia loadings. This approach offers a good state of dispersion of zirconia in the rubber matrix, along with enhanced zirconia–rubber interfacial interactions, compared to zirconia-filled NBR composites prepared by the conventional external addition of zirconia through two-roll milling. The thermal, mechanical, dynamic mechanical, curing and other properties of all the composites were comprehensively evaluated and comparatively analyzed to elucidate the effectiveness of the masterbatch-assisted *in situ* zirconia incorporation approach in enhancing the performance of zirconia-filled NBR composites.

2. Experimental

2.1. Materials

Nitrile butadiene rubber (34% acrylonitrile content and KNB-35L grade) was purchased from Rajchem (Mumbai, India). A solution of zirconium(IV) propoxide (zirconia precursor, 70% in 1-propanol) was procured from Sigma Aldrich (India). Toluene and tetrahydrofuran (THF) (purity $\geq$99%) were bought from Fisher Scientific Ltd (India). Zirconia powder (purity 98%, particle size 11–39 μm) was obtained from Loba Chem., India. Curing ingredients were supplied by Indian Rubber Materials Research Institute, Thane, Mumbai.

2.2. Preparation of composites

First, we prepared an *in situ* zirconia (40 phr) filled NBR composite following a reported method.[13] This composite was used as the masterbatch. For this purpose, 100 g of NBR fragments were dissolved in 800 mL of tetrahydrofuran (THF). The solution was then stirred, after which 146 ml of the zirconia precursor (zirconium(IV) propoxide solution) was added. Subsequently, 16 mL of water was added, and the mixture was continuously stirred for 1 h. The mixture was then subjected to a four-day period of gelation, followed by vacuum-drying of the gel at 80 °C. Next, for the preparation of the 5 phr zirconia containing composite (NBR-M-5-Zr), 17.5 g of the above stock was mixed with 87.5 g of raw NBR on a two-roll mill for a duration of 5 min. After this, the curing compounds were incorporated (Table 1). Mixing was continued until a homogeneous mixture was obtained, and finally, the mixture was cured at 160 °C in a mold according to its cure time (obtained from the curing study). This gave 5 g of zirconia per 100 g of NBR in the resultant composite, which is designated as NBR-M-5-Zr. In the same manner, the composites NBR-M-10-Zr and NBR-M-20-Zr were also prepared. Here, the letter M in the sample code represents masterbatch-derived rubber composites.

Unfilled and NBR-Ex-20-Zr composites were also prepared for comparison purposes. The NBR-Ex-20-Zr composite was prepared by masticating 100 g of raw NBR on a two-roll mill for 2 min. Next, 20 g of commercial zirconia was added, followed by compounding with crosslinking ingredients.

Table 1 Formulation of rubber composites expressed in phr (parts per hundred parts by weight of rubber)

Sample code	Unfilled	Stock	NBR-M-5-Zr	NBR-M-10-Zr	NBR-M-20-Zr	NBR-Ex-20-Zr
NBR	100	100	100	100	100	100
In situ zirconia	—	40	—	—	—	—
Master batch zirconia	—	—	5	10	20	—
Ex situ zirconia	—	—	—	—	—	20

Curing ingredients (in phr): ZnO: 5, stearic acid: 2, MBTS: 1.5, sulfur: 3.

A similar procedure without the addition of filler was adopted to prepare the unfilled NBR composite. All the composites were then cured on a hot press at 160 °C in a mold, according to their respective curing times.

2.3. Characterization

Cure characteristics were studied using a MDR Xgen100 moving die rheometer. Samples were subjected to a sinusoidal strain amplitude of 0.5° at a constant frequency of 1.66 Hz and a temperature of 160 °C, in accordance with the ISO 6502-2 standard. The reinforcing potential of the zirconia (α_f) was calculated using the following equation:[14]

$$\alpha_f = \left(\frac{\Delta M_f/\Delta M_0 - 1}{w}\right) \quad (1)$$

Here, ΔM_0 and ΔM_f represent the torque differences for the unfilled and filled rubber composites, respectively, and w denotes the weight fraction of zirconia in the rubber compound. X-ray diffraction (XRD) analysis was performed at room temperature using a Bruker D8 AVANCE diffractometer with Cu-Kα radiation (λ = 1.5406 Å) over a 2θ range of 5–90°. Scanning electron microscopy (SEM) was carried out using a field-emission SEM instrument (Zeiss EVO 18 Special Edition) with a working distance of 5 mm and an accelerating voltage of 5–10 kV. An Oxford INCAX-ACT, a sophisticated analytical instrument, was utilized for the precise identification of specific elements present within the composites under investigation. Stress–strain measurements were performed on a universal testing machine (H10KT, Tinius Olsen, UK) using ASTM D412 dumbbell specimens, a 500 N load cell, and a crosshead speed of 200 mm min^{-1} at ambient temperature, in accordance with ISO 527. The hardness measurements were conducted using a Shore A durometer (BSE Testing Machine, India) in accordance with ASTM D2240. The crosslink density (ν) was determined from equilibrium swelling measurements using the Flory–Rehner equation.[14,25] The viscoelastic strain sweep behavior of the uncured NBR composites was evaluated using a Rubber Process Analyzer (RPA 2000, Alpha Technologies) at 100 °C and 1.7 Hz over a strain range of 0.25–300%.

The circular samples were subjected to compression set study as per the ASTM D 395 standard for a duration of 24 h at 100 °C. A Stell spacer was used during the experiment to provide the recommended compression. The compression set percentage was calculated using the following formula:

$$\frac{t_0 - t_i}{t_0 - t_s} \times 100 \quad (2)$$

where t_i and t_0 are the final and initial thickness of the sample, respectively, and t_s is the height (in mm) of the spacer used.

Thermal analysis was performed using a TG-DTA analyzer (TG-DTA 7200, Hitachi, Japan) from 40 to 800 °C at a heating rate of 10 °C min^{-1} under nitrogen atmosphere. The glass transition temperature (T_g) was obtained from DSC measurement (DSC 204 F1, NETZSCH, Germany) after preheating the samples to 200 °C, cooling to −40 °C, and scanning from −35 to 35 °C at 5 °C min^{-1}. Dynamic mechanical analysis was conducted using a DMA (Eplexor 2000 N, Gabo Qualimeter, Germany) over −50 to 50 °C at 10 Hz and 2 °C min^{-1}. Aging resistance was evaluated following ISO 37 by aging specimens at 100 °C for 72 h and comparing the mechanical properties of aged and unaged samples.

3. Results and discussion

In this work, we first prepared an *in situ* zirconia-filled NBR composite following a reported method,[13] in which the zirconia content was 40 phr (parts per hundred parts by weight of rubber). This was utilized as a stock or masterbatch. Then, a calculated amount of this zirconia-containing NBR masterbatch was mixed with unfilled NBR in a suitable proportion to prepare 5, 10 and 20 phr zirconia-containing NBR composites. Two other composites were prepared for comparison purposes (unfilled NBR and an externally zirconia-filled composite (NBR-Ex-20-Zr). In-depth characterization of the composites was carried out, and the results have been analyzed and interpreted in the following section.

3.1. Curing study of zirconia-filled NBR composites

The rheological behavior of all composites is summarized in Table 2 and Fig. 1(a). The minimum torque (M_L) and maximum torque (M_H) are directly related to the viscosity and modulus of the rubber composites, respectively, while the Δ torque (R_∞) is directly related to the crosslinking density of the rubber composites.[10,19] All the zirconia-filled NBR composites show enhanced M_L, M_H, and R_∞ values compared with the unfilled rubber. Furthermore, at the same zirconia content, the values are higher for the masterbatch-derived composite (NBR-M-20-Zr) than for the externally zirconia-filled composite (NBR-Ex-20-Zr). The cure time also is influenced by the filler incorporation technique, and was found to be longer for the masterbatch-derived composite than the externally filled composite at same zirconia content. It can be noted that the trend of increasing cure time and decreasing cure rate index (CRI) with the

Table 2 Curing data of unfilled and zirconia-filled NBR composites

Sample code	Unfilled	NBR-M-5-Zr	NBR-M-10-Zr	NBR-M-20-Zr	NBR-Ex-20-Zr
Minimum torque (M_L) (dNm)	1.09	1.09	2.29	4.57	1.19
Maximum torque (M_H) (dNm)	12.83	23.37	34.90	37.28	15.41
Δ torque (R_∞) (dNm)	11.74	22.28	31.61	32.71	14.22
Cure time (t_{90}) (min)	9.32	14.06	15.39	23.36	11.32
Cure rate index (CRI)	13.98	8.10	6.96	4.51	11.94
Reinforcing potential (α_f)	—	18.86	18.62	10.71	2.32

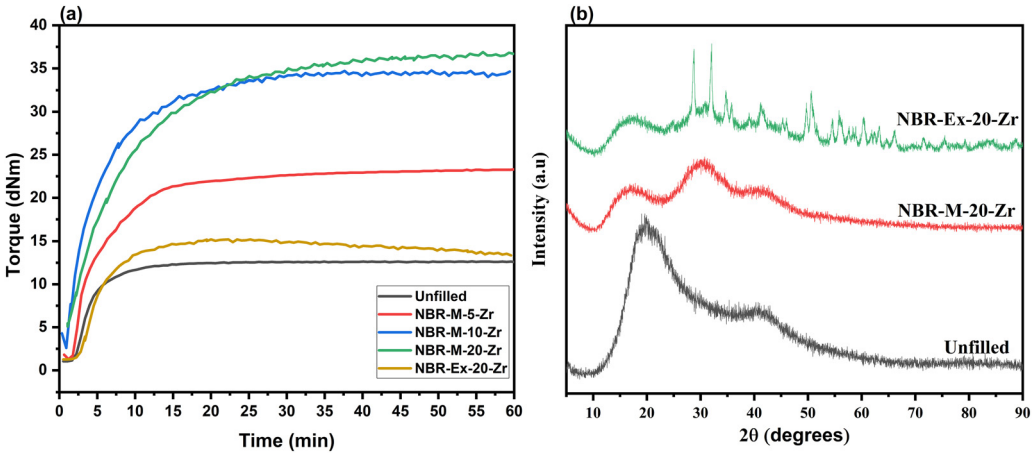

Fig. 1 (a) Curing behaviour and (b) X-ray diffraction patterns of an unfilled and NBR composites filled with zirconia.

addition of zirconia is similar to that observed in our earlier work.[13] Additionally, the value of reinforcing potential calculated using eqn (1) was found to be maximum for NBR-M-20-Zr, which was 5 times higher than that of NBR-Ex-20-Zr. Therefore, the results of the rheological study indicate that composites synthesized using the masterbatch approach demonstrate better rheological performance. A detailed study was conducted to validate this improvement and is discussed in the subsequent section.

3.2. Physical state of zirconia in the rubber matrix

The physical state of the zirconia, as well as its distribution in the elastomeric matrix, play vital roles in determining the final properties of the composites.[36] This was investigated for selected uncured samples using the XRD and FE-SEM techniques. In general, the sol–gel process yields amorphous zirconia, which can be transformed into a crystalline phase upon suitable heat treatment (calcination).[37,38] As shown in Fig. 1(b), the *in situ* generated zirconia is amorphous in nature in the composite NBR-M-20-Zr synthesized by masterbatch approach. Notably, the change in the hump position with the addition of zirconia relative to unfilled NBR in the XRD curve indicates the presence of amorphous zirconia in rubber matrix. A similar type of observation was reported in our earlier publication.[13] Notably, in case of the externally zirconia-filled composite, in which zirconia was added by external mixing, the zirconia is clearly seen to be crystalline in nature.

The distribution of zirconia and its size in the NBR composites prepared using the two different approaches were examined for selected samples *via* FE-SEM micrographs, which are presented in Fig. 2. In the micrographs, the zirconia particles are seen as bright spots against the dark region representing the NBR matrix. Notably, a more uniform dispersion of zirconia with negligible agglomeration is observed in the case of the composite prepared using the masterbatch approach (NBR-M-20-Zr) (Fig. 2a). In contrast, the externally filled composite (NBR-Ex-20-Zr) shows poor dispersion of zirconia with the appearance of large aggregates (Fig. 2b). As expected, the masterbatch-derived composite shows better dispersion of zirconia than the externally filled composite at the same filler

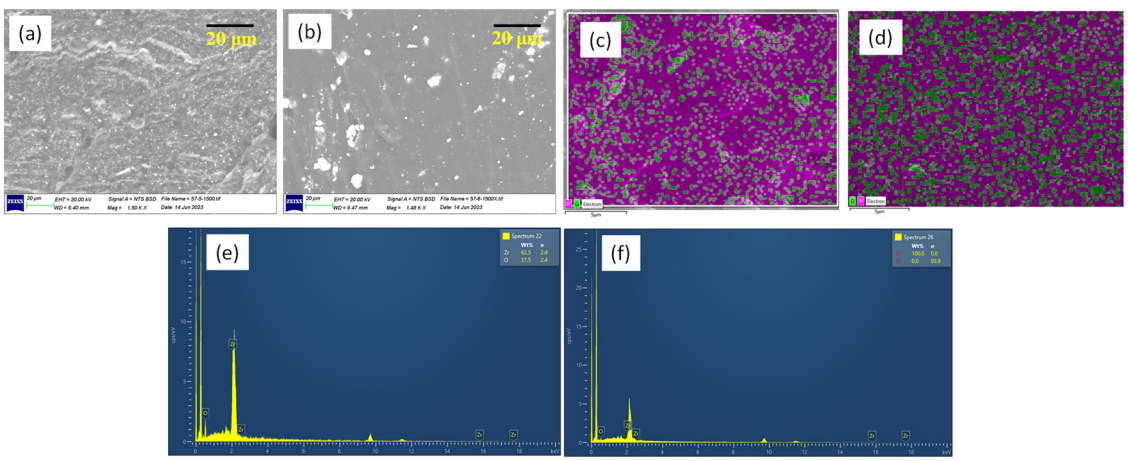

Fig. 2 FE-SEM micrographs of (a) NBR-M-20-Zr and (b) NBR-Ex-20-Zr. Elemental mapping images of (c) NBR-M-20-Zr and (d) NBR-Ex-20-Zr. EDX spectra of (e) NBR-M-20-Zr and (f) NBR-Ex-20-Zr.

Table 3 Stress–strain data of unfilled and zirconia-filled NBR composites

Sample code	Unfilled	NBR-M-5-Zr	NBR-M-10-Zr	NBR-M-20-Zr	NBR-Ex-20-Zr
$\sigma_{50\%}$ (MPa)	0.512 ± 0.04	0.516 ± 0.05	0.880 ± 0.02	0.987 ± 0.11	0.364 ± 0.05
$\sigma_{100\%}$ (MPa)	0.678 ± 0.02	0.920 ± 0.06	1.56 ± 0.07	2.10 ± 0.22	0.612 ± 0.04
$\sigma_{200\%}$ (MPa)	0.817 ± 0.02	1.50 ± 0.05	3.36 ± 0.12	5.04 ± 0.40	0.832 ± 0.04
$\sigma_{300\%}$ (MPa)	1.02 ± 0.01	2.15 ± 0.01	2.41 ± 0.51	7.01 ± 0.10	1.04 ± 0.05
Tensile strength (MPa)	1.41 ± 0.02	3.12 ± 0.10	4.16 ± 0.34	7.51 ± 0.05	2.00 ± 0.05
Elongation at break (%)	414 ± 6	399 ± 12	236 ± 12	281 ± 18	535.33 ± 26
Crosslinking density ($\upsilon \times 10^{-4}$)	3.64	5.47	7.78	8.20	5.27
Reinforcing efficiency (RE)	—	0.051	0.097	0.085	0.004
Mean hardness	30.4	36.8	37.4	46.6	33.4

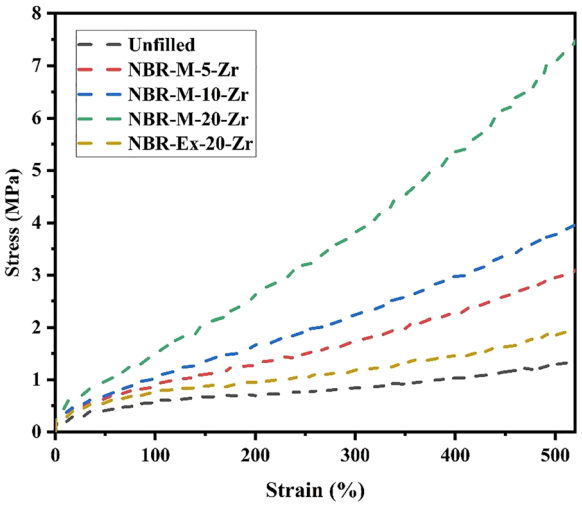

Fig. 3 Stress–strain curves of unfilled and zirconia-filled NBR composites.

content (Fig. 2c and d). The presence of zirconia in the composites was confirmed *via* EDX analysis, which revealed characteristic Zr and O peaks (Fig. 2e and f).

3.3. Mechanical response of rubber composites

In this section, an in-depth study of the stress–strain behaviour, viscoelastic behavior, and compression set of the composites is presented.

3.3.1. Stress–strain properties. The stress–strain results of the composites are presented in Table 3 and Fig. 3. All the zirconia-filled composites show an overall enhancement in tensile properties compared to unfilled NBR, confirming the reinforcing effect of zirconia. At a zirconia loading of 20 phr, the masterbatch-derived composite (NBR-M-20-Zr) exhibits higher moduli at low deformations ($\sigma_{50\%}$, $\sigma_{100\%}$, and $\sigma_{200\%}$) than the externally filled composite (NBR-Ex-20-Zr). Notably, NBR-M-20-Zr exhibits a tensile strength of 7.51 MPa, which is nearly four times higher than that of NBR-Ex-20-Zr. This is attributed to the uniform dispersion of the *in situ* generated zirconia and stronger rubber–filler interactions achieved through the masterbatch approach, enabling efficient stress transfer during deformation. However, the elongation at break of NBR-M-20-Zr is the lowest among the composites (281%), which can be correlated with its highest crosslink density (Table 3). The increased crosslink density leads to a stiffer network structure, thereby limiting chain extensibility and reducing overall deformability. This behavior is consistent with the reinforcement mechanism typically observed in *in situ* filled NBR composites.[13]

The reinforcing efficiency (RE)[16,19] was determined using eqn (3):

$$\mathrm{RE} = \frac{\sigma_{100\%_{filled}} - \sigma_{100\%\,unfilled}}{\mathrm{wt}_{\%_{filler}}} \quad (3)$$

where $\sigma_{100\%_{filled}}$ and $\sigma_{100\%_{unfilled}}$ are the 100% modulus of the zirconia-filled and unfilled composite, respectively.

As presented in Table 3, the *in situ* zirconia-filled composites show better reinforcing efficiency (RE) compared to the other samples, with NBR-M-20-Zr exhibiting a markedly higher RE than NBR-Ex-20-Zr at the same filler loading. In addition, the hardness increases consistently with the zirconia content in the masterbatch-derived composites, whereas the externally filled composite (NBR-Ex-20-Zr) shows a negligible effect. Notably, NBR-M-20-Zr exhibits the highest hardness among all samples.

3.3.2. Viscoelastic behaviour of the zirconia-filled rubber composites. Fig. 4 presents the viscoelastic behaviour of the composites as a function of strain. The dependence of the dynamic moduli on strain amplitude at a constant temperature and frequency is known as the Payne effect.[39] At higher strain levels, however, the rate of network destruction exceeds that of reassembly, leading to a reduction in storage modulus.[40] At lower strain, the filler–filler interactions are stronger and more dominant in the zirconia-filled composites, whereas at higher strain, these interactions are progressively suppressed, resulting in a steady decrease in modulus. As shown in Fig. 4(a), the masterbatch-derived composites show a considerable Payne effect, with the appearance of a maximum in the loss factor at a deformation level above 10 (Fig. 4(b)). Furthermore, the composite filled with 20 phr of zirconia (NBR-M-20-Zr) shows the highest Payne effect. On the other hand, the externally filled composite (NBR-Ex-20-Zr) with the same filler content shows a negligible Payne effect. This is due to the uneven distribution of zirconia for this composite.

3.3.3. Compression set study. Compression set is the permanent deformation of rubber composites, which measures its ability to retain elastic properties after prolonged compression under specified conditions. In general, a lower compression set indicates better elastic recovery and superior elastic properties of the material.[41,42] As shown in Fig. 5, both the masterbatch

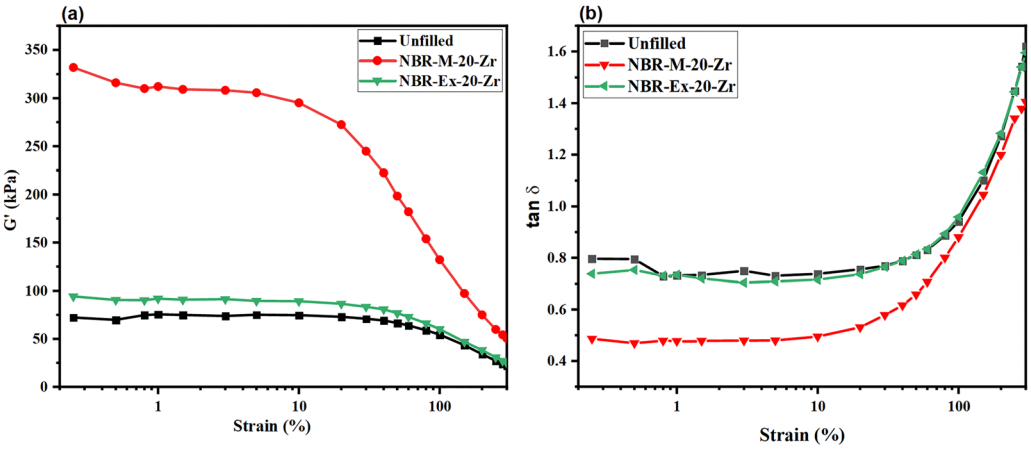

Fig. 4 (a) Storage modulus and (b) loss factor (tan δ) as a function of dynamic strain (%) for the unfilled and zirconia-filled NBR composites.

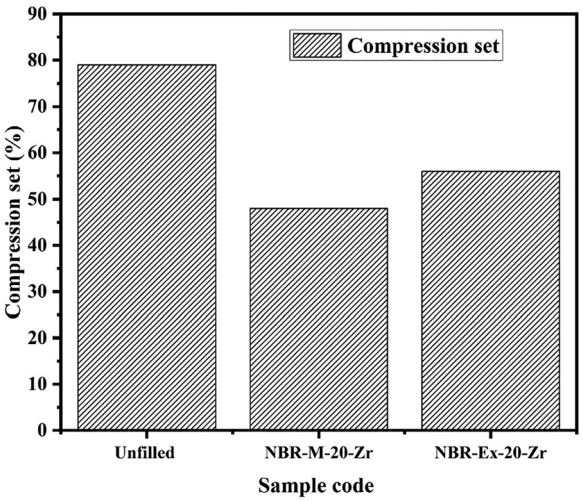

Fig. 5 Compression set of unfilled and zirconia-filled NBR composites.

derived and externally zirconia-filled composites at 20 phr show lower compression set than that of the unfilled NBR. However, the composite prepared *via* masterbatch approach (NBR-M-20-Zr) shows the lower value. Further, the higher value of compression set for the externally zirconia-filled composite (NBR-Ex-20-Zr) might be because of the poor interaction between rubber and zirconia as evidenced from morphological and other studies. Hence, it is very clear that the masterbatch-derived composite can better retain its elastic properties.

It is well established that the static compression set behaviour of NBR is strongly influenced by the filler type, loading, and dispersion quality. Several studies have indicated that fillers typically reduce compression set by restricting chain mobility and enhancing network stability. However, it should be noted that the improvement is not invariably monotonic. Carbon black-, silica-, and nanoclay-filled NBR composites demonstrate optimal reduction at suitable loadings. Conversely, excessive filler content or inadequate dispersion results in elevated permanent deformation.[42–44] The superior compression set performance of the masterbatch-derived zirconia-filled NBR composites observed in this work is in accordance with the trend of filled NBR composites reported in literature.[42–44] This highlights the critical role of the filler incorporation method and network integrity, rather than just the presence of filler alone.

3.4. Thermal behaviour of the rubber composites

3.4.1. Thermogravimetric study. The results of the thermogravimetric studies of unfilled and 20 phr-containing composites are shown in Table 4 and Fig. 6(a). The incorporation of zirconia into the NBR matrix enhances the thermal stability of the composites, which is reflected by the increase in both the onset degradation temperature (T_{onset}) and the temperature corresponding to maximum weight loss (T_{max}). These values are slightly higher for NBR-M-20-Zr compared to those of NBR-Ex-20-Zr. The enhanced thermal stability is achieved through the uniform dispersion of zirconia within the NBR matrix. Additionally, the refractory nature of zirconia facilitates its capacity to absorb and dissipate heat effectively, thereby retarding the thermal degradation of the rubber matrix.[45]

3.4.2. Differential scanning calorimetry (DSC). The glass transition temperatures (T_g) of the selected samples are summarized in Table 4 and illustrated in Fig. 6(b). An increase in T_g to −24.5 °C (NBR-M-20-Zr), compared to 28 °C for unfilled NBR, is evident in the composites prepared *via* the masterbatch approach. This increase in T_g is attributed to restricted segmental mobility of the rubber chains arising from the uniform dispersion of zirconia and enhanced rubber–filler interactions. Conversely, the externally filled composite demonstrates a decrease in T_g to −30.6 °C at an equivalent filler loading, which is indicative of inadequate filler dispersion and deficient interfacial interactions. Agglomerated zirconia particles exhibit

Table 4 Thermal data of unfilled and zirconia-filled NBR composites

Sample code	Unfilled	NBR-M-20-Zr	NBR-Ex-20-Zr
T_{onset} (°C)	407.5	412.7	411.4
T_{max} (°C)	438.5	457.7	455.7
T_g (°C)	−28.0	−24.5	−30.6

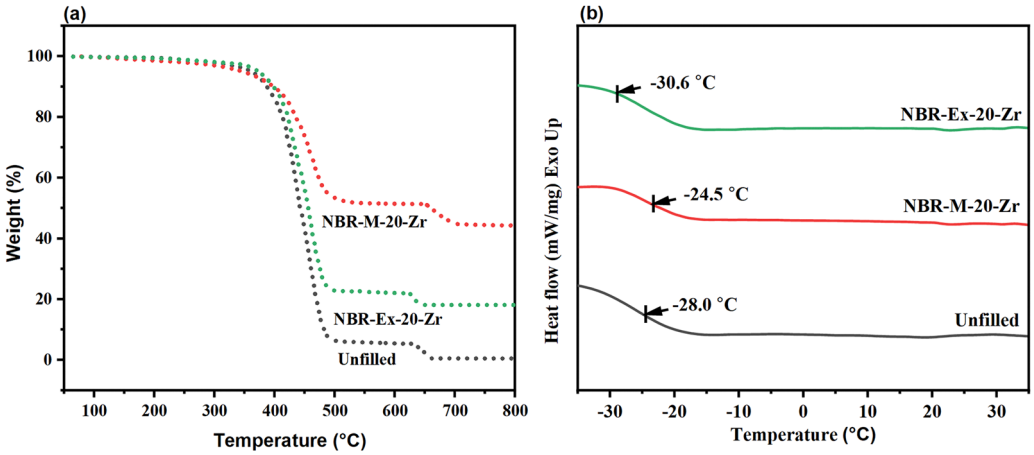

Fig. 6 (a) Thermograms and (b) DSC curves of unfilled and zirconia-filled NBR composites.

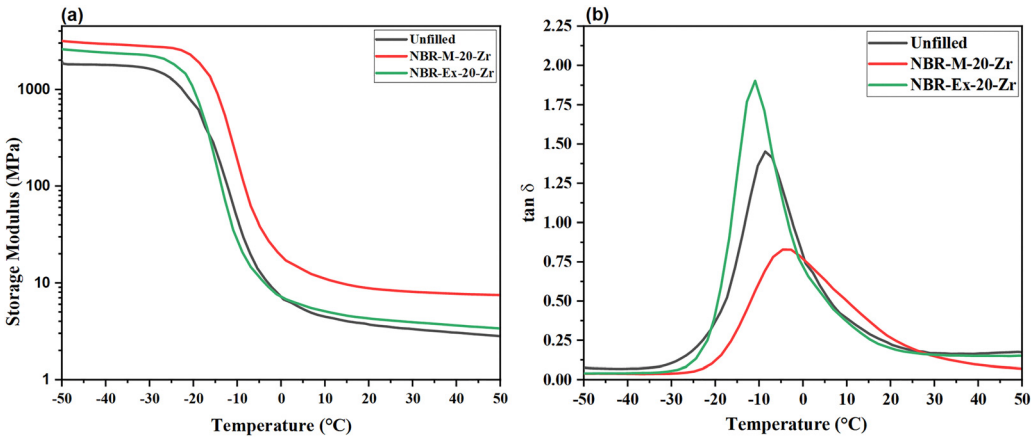

Fig. 7 (a) Storage modulus and (b) tan δ values of unfilled and zirconia-filled composites.

reduced efficacy in constraining polymer chain motion, potentially resulting in the formation of localized regions of increased free volume. This phenomenon has been observed to lead to a decrease in the glass transition temperature (T_g), a finding that aligns with prior studies on similar filler systems.[13,25]

3.5. Dynamic mechanical analysis (DMA)

The effect of zirconia loading on the dynamic performance of the composite, its reinforcing capability and rubber filler interaction were examined for selected composites using dynamic mechanical analysis (DMA). As observed in Fig. 7(a), at 20 phr of zirconia, the masterbatch derived *in situ* zirconia-filled composites exhibit a higher storage modulus compared to that of the unfilled and externally filled NBR composite in the rubbery region. This is the consequence of the even distribution of zirconia in the NBR matrix, as noted previously.

The temperature dependence of the loss tangent (tan δ) is presented in Fig. 7(b). The masterbatch-derived composite (NBR-M-20-Zr) exhibits a shift in the tan δ peak towards higher temperatures in comparison to unfilled NBR, indicating restricted segmental mobility due to the effective dispersion and enhanced reinforcing effect of the *in situ* generated zirconia. Furthermore, a reduction in the tan δ peak height is observed

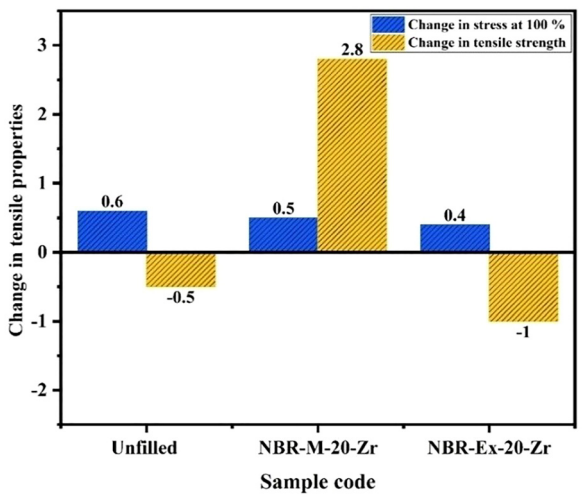

Fig. 8 Changes in tensile properties of unfilled and zirconia-filled NBR composites after aging.

relative to the unfilled sample, suggesting decreased energy dissipation. These results collectively indicate increased stiffness and elastic response in the masterbatch-prepared composite.[25]

3.6. Aging resistance study

The aging resistance of selected composites was evaluated by comparing their tensile properties before and after thermal aging. During the aging process, various chemical reactions, including crosslink formation, crosslink breakage, and polymer backbone scission, may occur, all of which directly influence the tensile behavior of rubber composites.[46,47] As shown in Fig. 8, the stress at $\sigma_{100\%}$ strain increases after aging, possibly because of further curing at high temperature.[48] However, the tensile strength after aging was found to increase only for the composite prepared *via* the masterbatch approach (NBR-M-20-Zr). A similar type of result was reported by our group for an *in situ* zirconia-filled rubber composite in which the tensile strength increases after aging.[16] This finding highlights the positive impact of the masterbatch approach on the aging performance.

4. Conclusions

In this study, the masterbatch approach was adopted to reinforce NBR with *in situ* incorporated zirconia. X-ray diffraction (XRD) analysis verified the amorphous nature of the *in situ* zirconia in the composite prepared by the masterbatch approach. Scanning electron microscopy (SEM) revealed that this approach facilitates a more uniform dispersion of zirconia within the NBR matrix compared to the externally filled composite. This results in substantial enhancements in mechanical and thermal properties, with the masterbatch-derived composite (NBR-M-20-Zr) demonstrating superior performance in comparison to its counterparts (NBR-Ex-20-Zr). In the rubbery region, this composite exhibits a higher storage modulus, indicating improved elasticity and network integrity. Additionally, a positive shift and reduction in the tan δ peak for NBR-M-20-Zr suggests lower energy dissipation and enhanced dynamic mechanical stability. Furthermore, NBR-M-20-Zr shows a good response in aging resistance and compression set studies, highlighting the practical applicability of such composites. Beyond performance metrics, this method offers a greener and more sustainable approach compared to the purely sol–gel-derived *in situ* filler incorporation method. It significantly reduces solvent and energy consumption, which are major environmental concerns in the conventional sol–gel process. Given its combined benefits of performance enhancement and process efficiency, the masterbatch method represents a promising scalable strategy for fabricating high-performance rubber composites. Future studies should focus on expanding this technique to other elastomer–filler systems, optimizing filler loadings, and conducting comprehensive physicochemical characterizations to enable broader industrial adoption.

Author contributions

Shubham C. Ambilkar: writing – original draft, visualization, methodology, investigation, data curation, conceptualization. Surabhi S. Raut: writing – review & editing, investigation, visualization, methodology, data curation, conceptualization. Bharat P. Kapgate: resources, data curation. Chayan Das: writing – review & editing, visualization, validation, supervision, resources, investigation, funding acquisition.

Conflicts of interest

There are no conflicts to declare.

Data availability

The data supporting this article are available from the corresponding author upon reasonable request.

Acknowledgements

Authors sincerely thank Department of Chemistry, VNIT Nagpur for providing a research platform. Special thanks to Dr Amit Das and Subhradeep Mandal for their assistance with DMA analysis.

References

1 K. Roy, S. C. Debnath and P. Potiyaraj, A critical review on the utilization of various reinforcement modifiers in filled rubber composites, *J. Elastomers Plast.*, 2020, **52**(2), 167.
2 B. P. Chang, A. Gupta, R. Muthuraj and T. H. Mekonnen, Bioresourced fillers for rubber composite sustainability: current development and future opportunities, *Green Chem.*, 2021, **23**(15), 5337.
3 Y. Fan, G. D. Fowler and M. Zhao, The past, present and future of carbon black as a rubber reinforcing filler–A review, *J. Cleaner Prod.*, 2020, **247**, 119115.
4 P. Dileep, G. A. Varghese, S. Sivakumar and S. K. Narayanankutty, An innovative approach to utilize waste silica fume from zirconia industry to prepare high performance natural rubber composites for multi-functional applications, *Polym. Test.*, 2020, **81**, 106172.
5 N. D. Bansod and C. Das, Studies on Mechanical, Rheological, Thermal, and Morphological Properties of In Situ Silica-Filled Butadiene Rubber Composites, *Plast., Rubber Compos.*, 2018, **47**(8), 345–351.
6 S. S. Sarkawi, W. Kaewsakul, K. Sahakaro, W. K. Dierkes and J. W. Noordermeer, A review on reinforcement of natural rubber by silica fillers for use in low-rolling resistance tires, *J. Rubber Res.*, 2015, **18**(4), 203.
7 S. Khanra, A. Kumar, S. K. Ghorai, D. Ganguly and S. Chattopadhyay, Influence of partial substitution of carbon black with silica on mechanical, thermal, and aging properties of super specialty elastomer based composites, *Polym. Compos.*, 2020, **41**(10), 4379.
8 C. Das, N. D. Bansod, B. P. Kapgate, K. Rajkumar and A. Das, Incorporation of titania nanoparticles in elastomer matrix to develop highly reinforced multifunctional

solution styrene butadiene rubber composites, *Polymer*, 2019, **162**, 1.
9 M. Ruan, D. Yang, W. Guo, L. Zhang, S. Li, Y. Shang, Y. Wu, M. Zhang and H. Wang, Improved dielectric properties, mechanical properties, and thermal conductivity properties of polymer composites via controlling interfacial compatibility with bio-inspired method, *Appl. Surf. Sci.*, 2018, **439**, 186.
10 D. Vijayan, A. Mathiazhagan and R. Joseph, Aluminium trihydroxide: Novel reinforcing filler in Polychloroprene rubber, *Polymer*, 2017, **132**, 143.
11 S. C. Ambilkar, T. Singal and C. Das, Diverse role of zirconia in developing polymeric composites, *Polym. Bull.*, 2024, **81**(8), 6641.
12 G. Garnweitner, Zirconia nanomaterials: synthesis and biomedical application. *Nanotechnologies for the Life Sciences*, 2009, vol. 10, p. 9783527610419.
13 S. C. Ambilkar, N. D. Bansod, B. P. Kapgate, A. Das, P. Formanek, K. Rajkumar and C. Das, In situ zirconia: A superior reinforcing filler for high-performance nitrile rubber composites, *ACS Omega*, 2020, **5**(14), 7751.
14 S. S. Raut, S. C. Ambilkar, B. P. Kapgate, A. Das, S. Mandal, A. K. Ghosh and C. Das, Moving beyond organosilanes: Tris (hydroxymethyl) aminomethane as a superior surface modifier for zirconia in NBR composites, *Polymer*, 2025, **328**, 128405.
15 C. Das, N. D. Bansod, B. P. Kapgate, U. Reuter, G. Heinrich and A. Das, Development of highly reinforced acrylonitrile butadiene rubber composites via controlled loading of sol-gel titania, *Polymer*, 2017, **109**, 25.
16 S. C. Ambilkar, G. L. Dhakar, B. P. Kapgate, A. Das, S. Hait, R. Gedam, R. Kasilingam and C. Das, Enhancing the material performance of chloroprene rubber (CR) by strategic incorporation of zirconia, *Mater. Adv.*, 2022, **3**(5), 2434.
17 B. Huang, Y. Yu, Y. Zhao, Y. Zhao, L. Dai, Z. Zhang and H. F. Fei, Effects of metal oxides on the dielectric and mechanical properties of silicone rubber composites, *J. Appl. Polym. Sci.*, 2024, **141**(8), e54983.
18 B. P. Kapgate, C. Das, D. Basu, A. Das, G. Heinrich and U. Reuter, Effect of silane integrated sol–gel derived in situ silica on the properties of nitrile rubber, *J. Appl. Polym. Sci.*, 2014, **131**, 15.
19 S. C. Ambilkar and C. Das, Surface modification of zirconia by various modifiers to investigate its reinforcing efficiency toward nitrile rubber, *Polym. Compos.*, 2023, **44**(3), 1512.
20 P. S. Sarath, S. Thomas, J. T. Haponiuk and S. C. George, Fabrication, characterization and properties of silane functionalized graphene oxide/silicone rubber nanocomposites, *J. Appl. Polym. Sci.*, 2022, **139**(30), e52299.
21 K. Roy, S. C. Debnath, D. Basu, A. Pongwisuthiruchte and P. Potiyaraj, Emerging advances in rubber technology by the suitable application of sol-gel science and technology, *Rubber Chem. Technol.*, 2021, **94**(4), 601.
22 S. Utrera-Barrios, R. Perera, N. León, M. H. Santana and N. Martínez, Reinforcement of natural rubber using a novel combination of conventional and in situ generated fillers, *Compos., Part C: Open Access*, 2021, **5**, 100133.
23 L. Strohmeier, B. Schrittesser and S. Schlögl, Approaches toward in situ reinforcement of organic rubbers: Strategy and recent progress, *Polym. Rev.*, 2022, **62**(1), 142.
24 L. Wahba, M. D'Arienzo, R. Donetti, T. Hanel, R. Scotti, L. Tadiello and F. Morazzoni, In situ sol–gel obtained silica–rubber nanocomposites: influence of the filler precursors on the improvement of the mechanical properties, *RSC Adv.*, 2013, **3**(17), 5832.
25 S. C. Ambilkar, B. P. Kapgate, A. Das, S. Mandal, P. K. Maji, S. Singh, R. Kasilingam, R. S. Gedam and C. Das, Precise role of zirconia to boost up the mechanical, thermal, viscoelastic, dielectric, and chemical resistance properties of natural rubber-nitrile rubber blend, *Eur. Polym. J.*, 2023, **194**, 112163.
26 K. Buaksuntear, N. Choosang, K. Mougin, A. Spangenberg, A. Le Duigou and W. Smitthipong, Recent advancements in masterbatch filler technology and filler dispersion for rubber and polymer composites: a review, *Polym. Eng. Sci.*, 2025, 1–29.
27 V. S. Raman, A. Das, K. Stöckelhuber, S. Eshwaran, J. Chanda, M. Malanin, U. Reuter, A. Leuteritz, R. Boldt and S. Wießner, Improvement of mechanical performance of solution styrene butadiene rubber by controlling the concentration and the size of in situ derived sol–gel silica particles, *RSC Adv.*, 2016, **6**(40), 33643.
28 A. Adibi, D. Jubinville, G. Chen and T. H. Mekonnen, In-situ surface grafting of lignin onto an epoxidized natural rubber matrix: a masterbatch filler for reinforcing rubber composites, *React. Funct. Polym.*, 2024, **197**, 105856.
29 S. S. Nair, T. Saha, V. K. Arya and S. Bhadra, A novel economically viable method of preparation of graphene–rubber masterbatch for its application in tyre compound, *Mater. Today: Proc.*, 2022, **62**, 7113–7117.
30 J. Yang, B. Xian, H. Li, L. Zhang and D. Han, Preparation of silica/natural rubber masterbatch using solution compounding, *Polymer*, 2022, **244**, 124661.
31 J. Tan, X. Wang, Y. Luo and D. Jia, Rubber/clay nanocomposites by combined latex compounding and melt mixing: A masterbatch process, *Mater. Des.*, 2012, **34**, 825–831.
32 Y. Qiu, A. Zhang and L. Wang, Carbon black–filled styrene butadiene rubber masterbatch based on simple mixing of latex and carbon black suspension: preparation and mechanical properties, *J. Macromol. Sci., Part B: Phys.*, 2015, **54**(12), 1541–1553.
33 M. Balachandran and S. S. Bhagawan, Mechanical, thermal, and transport properties of nitrile rubber–nanocalcium carbonate composites, *J. Appl. Polym. Sci.*, 2012, **126**(6), 1983–1992.
34 M. Balachandran and S. S. Bhagawan, Mechanical, thermal and transport properties of nitrile rubber (NBR)–nanoclay composites, *J. Polym. Res.*, 2012, **19**(2), 9809.
35 G. Zhou, K. Wu, W. Pu, P. Li and Y. Han, Tribological modification of hydrogenated nitrile rubber nanocomposites for water-lubricated bearing of ship stern shaft, *Wear*, 2022, **504**, 204432.
36 J. Wang, L. Yang, J. Xie, Y. Wang and T.-J. Wang, Surface amination of silica nanoparticles using tris (hydroxymethyl) aminomethane, *Ind. Eng. Chem. Res.*, 2020, **59**(49), 21383.

37 O. Stachs, T. Gerber and V. Petkov, The structure formation of zirconium oxide gels in alcoholic solution, *J. Sol-Gel Sci. Technol.*, 1999, **15**, 23.
38 E. S. Junior, S. Antonio and E. Longo, Synthesis and structural evolution of partially and fully stabilized ZrO2 from a versatile method aided by microwave power, *Ceram. Int.*, 2018, **44**(3), 3517.
39 H. Xu, X. Fan, Y. Song and Q. Zheng, Reinforcement and Payne effect of hydrophobic silica filled natural rubber nanocomposites, *Compos. Sci. Technol.*, 2020, **187**, 107943.
40 R. Yang, Y. Song and Q. Zheng, Payne effect of silica-filled styrene-butadiene rubber, *Polymer*, 2017, **116**, 304.
41 K. Pal, R. Rajasekar, D. J. Kang, Z. X. Zhang, S. K. Pal, C. K. Das and J. K. Kim, Effect of fillers on natural rubber/high styrene rubber blends with nano silica: morphology and wear, *Mater. Des.*, 2010, **31**(2), 677.
42 A. Mostafa, A. Abouel-Kasem, M. Bayoumi and M. El-Sebaie, Effect of carbon black loading on the swelling and compression set behavior of SBR and NBR rubber compounds, *Mater. Des.*, 2009, **30**(5), 1561.
43 K. Senthilvel, S. Vishvanathperumal, B. Prabu and L. John Baruch, Studies on the morphology, cure characteristics and mechanical properties of acrylonitrile butadiene rubber with hybrid filler (carbon black/silica) composite, *Polym. Polym. Compos.*, 2016, **24**(7), 473–480.
44 S. Pashaei, S. Hosseinzadeh and A. A. Syed, Studies on coconut shell powder and crys-nanoclay incorporated acrylonitrile–butadiene rubber/styrene–butadiene rubber (NBR/SBR) green nanocomposites, *Polym. Compos.*, 2017, **38**(4), 727–735.
45 A. Karaulov, T. Piskun and N. Kvasman, Physical and mechanical properties of zirconium dioxide refractories and their resistance to attack by molten metals, *Refractories*, 1993, **34**(7), 367.
46 F.-Z. Li, M.-R. Gao, B. Guo and N. Bolf, Investigation of ageing behaviour of nitrile-butadiene rubber with added graphene in an accelerated thermal ageing environment, *Kem. Ind.*, 2018, **67**(1–2), 29.
47 A. Mostafa, A. Abouel-Kasem, M. Bayoumi and M. El-Sebaie, The influence of CB loading on thermal aging resistance of SBR and NBR rubber compounds under different aging temperature, *Mater. Des.*, 2009, **30**(3), 791.
48 J. Diez, R. Bellas, J. López, G. Santoro, C. Marco and G. Ellis, Study of the crosslink density, dynamo-mechanical behaviour and microstructure of hot and cold SBR vulcanizates, *J. Polym. Res.*, 2010, **17**, 99.